




Geophysical Research Letters®



RESEARCH LETTER

10.1029/2023GL107050

Seasonality in Carbon Flux Attenuation Explains Spatial Variability in Transfer Efficiency

Francisco de Melo Viríssimo^{1,2} , Adrian P. Martin¹ , Stephanie A. Henson¹ , and Jamie D. Wilson^{3,4} 

¹National Oceanography Centre, Southampton, UK, ²Grantham Research Institute on Climate Change and the Environment, London School of Economics and Political Science, London, UK, ³School of Earth Sciences, University of Bristol, Bristol, UK, ⁴Department of Earth, Ocean and Ecological Sciences, University of Liverpool, Liverpool, UK

Key Points:

- Spatial variability in carbon transfer efficiency (TE) can be generated solely by the seasonality of flux attenuation informed by observations
- Seasonality in flux attenuation can reconcile contrasting TE maps reported in the literature
- Resolving and understanding seasonality are key for an accurate evaluation of the biological carbon pump under climate change

Supporting Information:

Supporting Information may be found in the online version of this article.

Correspondence to:

F. de Melo Viríssimo,
f.de-melo-virissimo@lse.ac.uk

Citation:

de Melo Viríssimo, F., Martin, A. P., Henson, S. A., & Wilson, J. D. (2024). Seasonality in carbon flux attenuation explains spatial variability in transfer efficiency. *Geophysical Research Letters*, 51, e2023GL107050. <https://doi.org/10.1029/2023GL107050>

Received 27 OCT 2023

Accepted 26 JAN 2024

Author Contributions:

Conceptualization: Francisco de Melo Viríssimo

Data curation: Francisco de Melo Viríssimo

Formal analysis: Francisco de Melo Viríssimo, Jamie D. Wilson

Funding acquisition: Adrian P. Martin, Stephanie A. Henson

Investigation: Francisco de Melo Viríssimo

Methodology: Francisco de Melo Viríssimo

Resources: Adrian P. Martin, Stephanie A. Henson

Software: Francisco de Melo Viríssimo

Validation: Francisco de Melo Viríssimo

Visualization: Francisco de Melo Viríssimo, Jamie D. Wilson

© 2024. The Authors.

This is an open access article under the terms of the [Creative Commons Attribution License](https://creativecommons.org/licenses/by/4.0/), which permits use, distribution and reproduction in any medium, provided the original work is properly cited.

Abstract Each year, the biological carbon pump (BCP) transports large quantities of carbon from the ocean surface to the interior. The efficiency of this transfer varies geographically, and is a key determinant of the atmosphere-ocean carbon dioxide balance. Traditionally, the attention has been focused on explaining perceived geographical variations in this transfer efficiency (TE) in an attempt to understand it, an approach that has led to conflicting results. Here we combine observations and modeling to show that the spatial variability in TE can instead be explained by the seasonal variability in carbon flux attenuation. We also show that seasonality can explain the contrast between known global estimates of TE, due to differences in the date and duration of sampling. Our results suggest caution in the mechanistic interpretation of annual-mean patterns in TE and demonstrates that seasonally and spatially resolved data sets and models might be required to generate accurate evaluations of the BCP.

Plain Language Summary Each year, marine phytoplankton convert carbon dioxide into millions of tonnes of organic carbon with a fraction of it reaching the deep ocean, where it can remain for hundreds of years. The efficiency of this surface-to-depth carbon transfer is therefore a key determinant of the atmosphere-ocean carbon dioxide balance. However, the variability of this transfer efficiency (TE) and its underlying causes are poorly understood, to the extent that different studies report contradicting results. We show that the existence of seasonal variability in the attenuation of sinking carbon particles can explain the observed spatial variability in annual TE and reconcile with the literature. Our findings suggest caution in interpreting results from sparse but time-varying data sets, highlighting that seasonal variability should be considered when studying the oceanic carbon cycle.

1. Introduction

The biological carbon pump (BCP) plays a crucial role in the ocean's carbon cycle by removing large quantities of carbon dioxide (CO₂) from the surface ocean to the deep interior (Volk & Hoffert, 2013). In this process, marine phytoplankton assimilate dissolved CO₂ in the sunlit, upper ocean to produce around 50 Pg of organic carbon per year (Lima et al., 2014). While most organic carbon production is quickly respired back into inorganic carbon, about 10%–20% is “exported” into the mesopelagic ocean (100–1,000 m) as particulate organic carbon (POC), or detritus (Saba et al., 2021). Eventually, part of this POC reaches the deep, bathypelagic ocean (below 1,000 m), where it may remain for hundreds of years (DeVries et al., 2012) before returning to the surface ocean as dissolved inorganic carbon. Through this process, the BCP is estimated to sequester over 1,280 Pg C at steady state (Nowicki et al., 2022), and in this way lowering the baseline atmospheric concentration of CO₂ by more than 50% with respect to the effects of physical and chemical equilibrium alone (Maier-Reimer et al., 1996).

In this biogeochemical journey, there are essentially two contrasting processes which determine the fate of the exported POC: sinking and remineralization (Middelburg, 2019). As POC sinks downward, it is remineralized by being broken down and respired by heterotrophic organisms. It is the balance between these processes (which may also include coupling (Alcolombri et al., 2021)) that determines the efficiency of the BCP in transferring POC to the deep ocean. For a given remineralization rate, the faster the POC sinks, the more of it will survive the journey, with a higher fraction reaching the deep ocean. The “TE” (hereafter TE) is defined as the ratio between the POC flux at 1,000 m divided by the export flux.

Writing – original draft: Francisco de Melo Viríssimo

Writing – review & editing: Francisco de Melo Viríssimo, Adrian P. Martin, Stephanie A. Henson, Jamie D. Wilson

In practice, TE is usually derived from particle flux profiles by applying a function to describe the decrease of flux with depth; the most popular function is the “Martin curve” (Martin et al., 1987; Middelburg, 2019). This formulation states that TE equals the ratio of the export depth and the transfer depth to the power of an exponent, hereafter b , where the exponent b can be estimated from flux profiles (Supporting Information S1). From a mechanistic point of view, b can be expressed as the ratio between sinking and remineralization rates (Equation 14 in Supporting Information S1). For this reason, b is usually referred to as the flux attenuation exponent. Since the proposal of such parameterizations for the BCP, they have been widely used in both data and model-based studies, often with the flux attenuation exponent assuming Martin’s original value of $b = 0.858$ (Martin et al., 1987).

Evidence from observation and model-based studies suggest the flux attenuation exponent, and therefore TE, is significantly variable though. For instance, a series of independent field-based investigations (Berelson, 2001; Buesseler et al., 2007; Conte et al., 2001; Francois et al., 2002; Lutz et al., 2002) estimated values of b between 0.5 and 2.0 across the ocean, later used as the basis to assess the influence of remineralization depth changes on atmospheric pCO₂ (Kwon et al., 2009; Wilson et al., 2019). Several global compilations for TE to be proposed over the years, with two of them standing out: a compilation of Thorium-derived export fluxes and sediment-trap fluxes at 2,000 m (Henson et al., 2012), which found TE to be lower at low latitudes and high at high latitudes, and a compilation obtained from a limited set of eight data points collected with neutrally buoyant mesopelagic sediment-traps from the North Atlantic and Pacific, which showed the opposite pattern (Marsay et al., 2015). Later studies using data-constrained modeling (Cram et al., 2018; DeVries & Weber, 2017; Weber et al., 2016) obtained TE distributions that agreed with the latter, but were not able to explain why they differ from the former. It is important to understand the source of such variability because the spatial patterns can be used to infer net dominant processes such as temperature-dependent remineralization or ballasting, which can then be used to make predictions of how carbon sequestration by the BCP may change as a response to climate-driven changes in those processes (Wilson et al., 2019).

More recently, additional evidence for seasonal variability in TE has been presented (Bol et al., 2018; Henson et al., 2023; Kienast & Torfstein, 2022), with subsequent implications for carbon sequestration. Numerical experiments showed that the adding a cosine-like seasonal variability of 60% (about the mean) in the flux attenuation parameter more than doubles the sequestration of carbon predicted by an ocean-biogeochemical model (de Melo Viríssimo et al., 2022), while an extensive sensitivity analysis performed by the same study showed that this increase is independent of the cycle’s peak (or, equivalently, its phase).

Here, we demonstrate the importance of resolving seasonality in the BCP with three key results: first, we leverage from an extensive data compilation of POC flux attenuation parameter values (Guidi et al., 2015) to constrain the mean seasonal cycle in each hemisphere, which is shown to approximate a cosine curve that peaks in spring as presented in Figure 1 and Figure S1 in Supporting Information S1. We then use a global ocean-biogeochemical model to link seasonal to spatial variability by showing that the presence of a seasonally varying but spatially uniform flux attenuation is, by itself, sufficient to generate spatial variability in TE, with a resulting global distribution of annual TE that agrees with those presented in the literature (Cram et al., 2018; DeVries & Weber, 2017; Marsay et al., 2015; Weber et al., 2016). Finally, we show that considering seasonality allows the reconciliation of the conflicting results for global annual TE spatial patterns discussed above (Henson et al., 2012; Marsay et al., 2015).

In what follows, we apply a uniform but seasonally varying flux attenuation informed by observations (Figure 1 and Figure S1 in Supporting Information S1) within a coupled global ocean-biogeochemical model. To allow a direct comparison between the constant and seasonal flux attenuation scenarios, as well as to remove uncertainties when computing TE, we assume that the POC is not transported by circulation and can only sink vertically. A detailed description of the model and underlying assumptions is presented in the Materials and Methods section and the Supporting Information S1.

2. Materials and Methods

2.1. Diagnostic Model

We use a coupled global ocean-biogeochemical model. The biogeochemical component is the GEOMAR NPZD-DOP model (Kriest et al., 2010, 2012). The biogeochemistry is coupled to the circulation via a transport-matrix

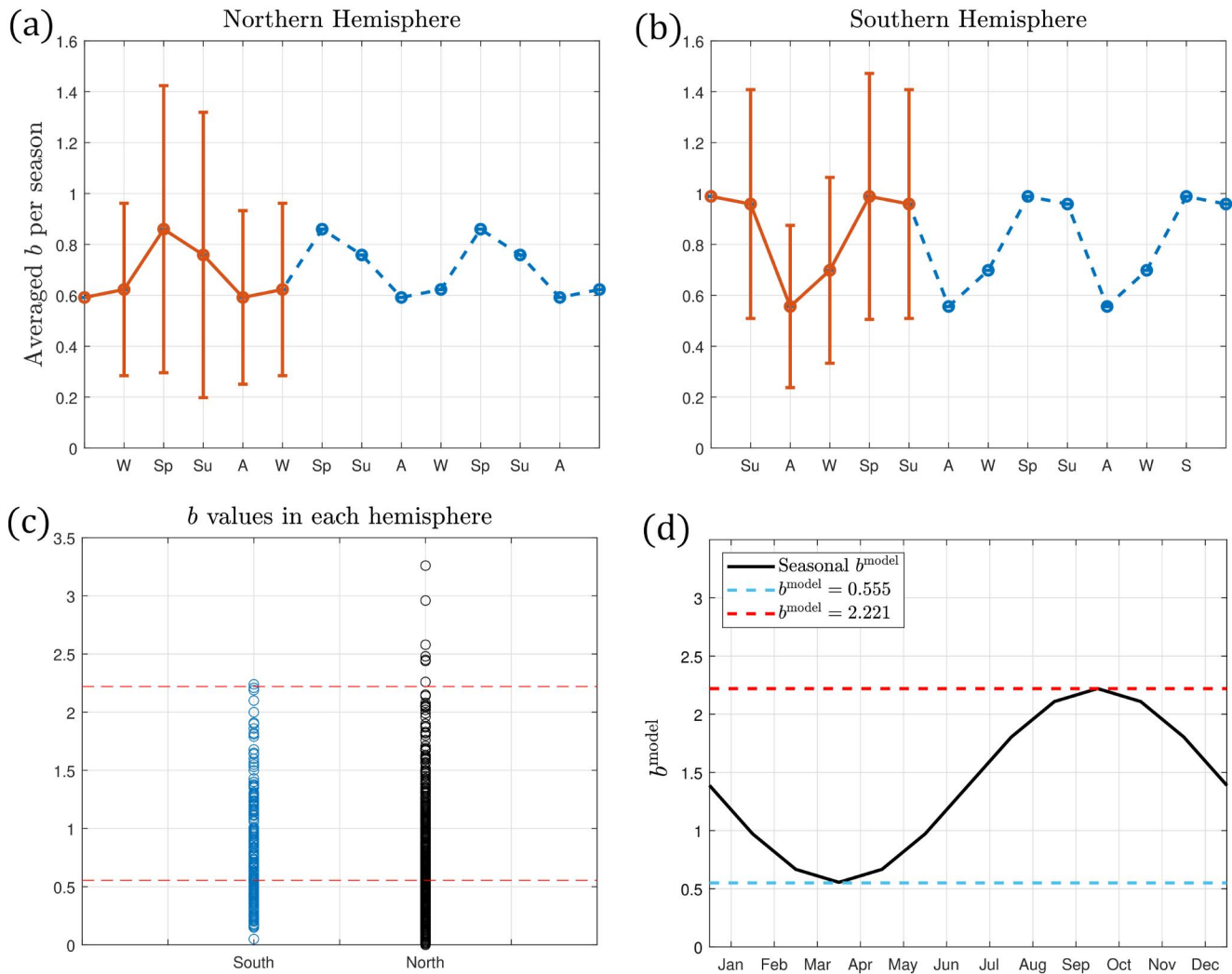


Figure 1. Constraining the seasonal cycle in the flux attenuation parameter b in each hemisphere from the UVP data set (Guidi et al., 2015). Top row: seasonally averaged flux attenuation parameter b in the Northern Hemisphere (a) and Southern Hemisphere (b). The solid red line shows one full seasonal cycle, while the blue dash line shows the cycle repeated, to highlight its sinusoidal pattern. Bottom row: (c) Distribution of b values from the UVP data set in each hemisphere. The dashed red line highlights the values of $b = 0.555$ and $b = 2.221$ (the minimum and maximum values used in this study); (d) Resulting seasonal b^{model} used in this study, shown here for the Southern Hemisphere.

(TMM) framework (Khatiwala, 2007, 2018; Khatiwala et al., 2005). For the circulation, we use 12 monthly averaged transport matrices derived from the MITgcm 2.8° (Khatiwala, 2018; Khatiwala et al., 2005). This model includes detritus explicitly as a tracer, which sinks at an intrinsic speed $w(z) = a \cdot z$ m day⁻¹, $a > 0$, and is remineralized at a constant rate $\lambda = 0.05$ days⁻¹. In the absence of circulation, the 1-year average fluxes are given by the Martin curve, with $b = \lambda/a$. To avoid confusion with the Martin curve, we denote the model's flux attenuation by b^{model} (de Melo Viríssimo et al., 2022). With the TMM, it is also possible to easily turn off circulation influence on detritus, and hence remove its effect on detritus transport (de Melo Viríssimo et al., 2022), this way allowing for a clean diagnostic of the effects of a seasonal flux attenuation. The latter is a crucial point in this study and, in all simulations, the ocean circulation does not act on the sinking detritus (but does act on all other tracers).

2.2. Seasonal Cycle

The model has been modified to incorporate seasonality in its flux attenuation by modifying its sinking speed: since $a = \lambda/b^{\text{model}}$, we replace b^{model} by a seasonally varying version constrained by observations (Guidi et al., 2015) as

per Figure 1 and Figure S1 in Supporting Information S1. This seasonal b^{model} has variability of 60% around the model's original reference value of $b^{\text{model}} = 1.388$ (Kriest et al., 2017), as shown in Figure 1d and Figure S3 in Supporting Information S1. This covers the range of observed values from about 0.5 to 2.0 (Kwon et al., 2009), as shown in Figure 1c, while excluding very low values (below 0.5) which, in our model, would lead to unrealistically fast sinking of POC. The phase (with respect to 1st of January) was also constrained from observations, as shown in Figures 1a and 1b), and is approximately 3 months ahead of growth rate of phytoplankton and solar radiation (Supporting Information S1). The former means that fastest sinking (lowest attenuation and highest TE) happens between February and May, which occurs about 3 months after maximum growth (as suggested by North Atlantic glider data (Bol et al., 2018)). This phase is also within the uncertainty margin reported from annual sediment trap data for the North Red Sea (Kienast & Torfstein, 2022). Note that the seasonal b^{model} is spatially homogeneous at each instant of time, so there is no spatial variability in b^{model} nor in sinking speed at each depth.

3. Results and Discussion

3.1. Seasonality Leads to Spatial Variability in Annual Transfer Efficiency

In the absence of seasonal variability in the model's flux attenuation b^{model} and sinking speed (see Materials and Methods and Supporting Information S1), the annual mean TE is spatially invariant throughout the ocean. This is shown in Figure S4 in Supporting Information S1 for the model's original value of $b^{\text{model}} = 1.388$, which means that $TE \approx 0.04738$ as predicted by the Martin curve (see Supporting Information S1). When seasonality in attenuation and sinking speed is present (Figure 2a), the annual mean TE is no longer homogeneous and shows a broad spatial pattern of values ranging from approximately 0.15–0.3 in the Southern Ocean, North Atlantic and North Pacific, and 0.05–0.15 in the subtropical gyres and tropical areas. The consistent spatial pattern of high TE at high latitudes and low at low latitudes, particularly in the subtropics, is in agreement with previous attempts to estimate TE using a variety of methods such as data-constrained modeling (DeVries & Weber, 2017; Weber et al., 2016), large-scale mechanistic modeling (Cram et al., 2018) and from neutrally buoyant sediment traps (Marsay et al., 2015). The exception is the pattern obtained from deep-sea sediment and Thorium-derived export fluxes compilation analysis (Henson et al., 2012), which found TE to be higher in low latitudes than in high latitudes, a conclusion that we will examine further in the next section.

The annual mean TE in ocean provinces (Figure 2b; see Supporting Information S1 for the provinces division and flux calculations) shows that the Antarctic province AAZ and North Atlantic province NA have high values of TE (0.18 and 0.16 respectively), while the subtropical provinces STA and STP have the lowest values of 0.13 and 0.11 respectively, with all other provinces showing values in between. These estimates are in good qualitative agreement with previous modeling studies (Cram et al., 2018) and within the uncertainty margin of data-constrained modeling studies (DeVries & Weber, 2017; Weber et al., 2016) for all provinces but STP and NP in the Pacific Ocean, with the caveat that our province division is similar but slightly different (see Supporting Information S1). The annual global mean TE is 0.14, which also falls between the high and low latitude values in Figure 2a. However, it is slightly lower than the 0.15 given by the Martin curve when $b = 0.858$.

The emergence of a spatial pattern in TE in the model, despite having a spatially homogeneous flux attenuation, is a direct consequence of the seasonal variability in the attenuation. If the attenuation is invariant throughout the year, its effect on the sinking detritus concentrations (and fluxes) is simply to reduce the concentration of detritus with depth, but keeping the shape of the time series unchanged (Figure 3a), like a traveling wave under damping. Therefore, at different depths, the detritus concentration has the same seasonal cycle, but with an increasing lag relative to the export depth, as illustrated for a location in the South Atlantic in Figure 3c. Because this attenuation is constant at all locations, the ratio between the 1-year integral of the time series at any two depths below the export depth will be the same at any location (Figure 3a). If seasonality is present, the differing attenuation at different times of the year will alter the time series of flux at depth: for example, periods of higher flux from the surface may coincide with low attenuation in some locations, but with high attenuation in others. The deeper the depth horizon considered, the greater the lag with respect to the time series at the export depth, as shown in Figures 3b and 3d. As this distortion is dependent on the characteristics of the time series, the ratio between the 1-year integral of the time series at two depths below the export depth will be different at different locations. Examples of modeled time series in the Pacific and Indian Oceans are shown in Supporting Information S1.

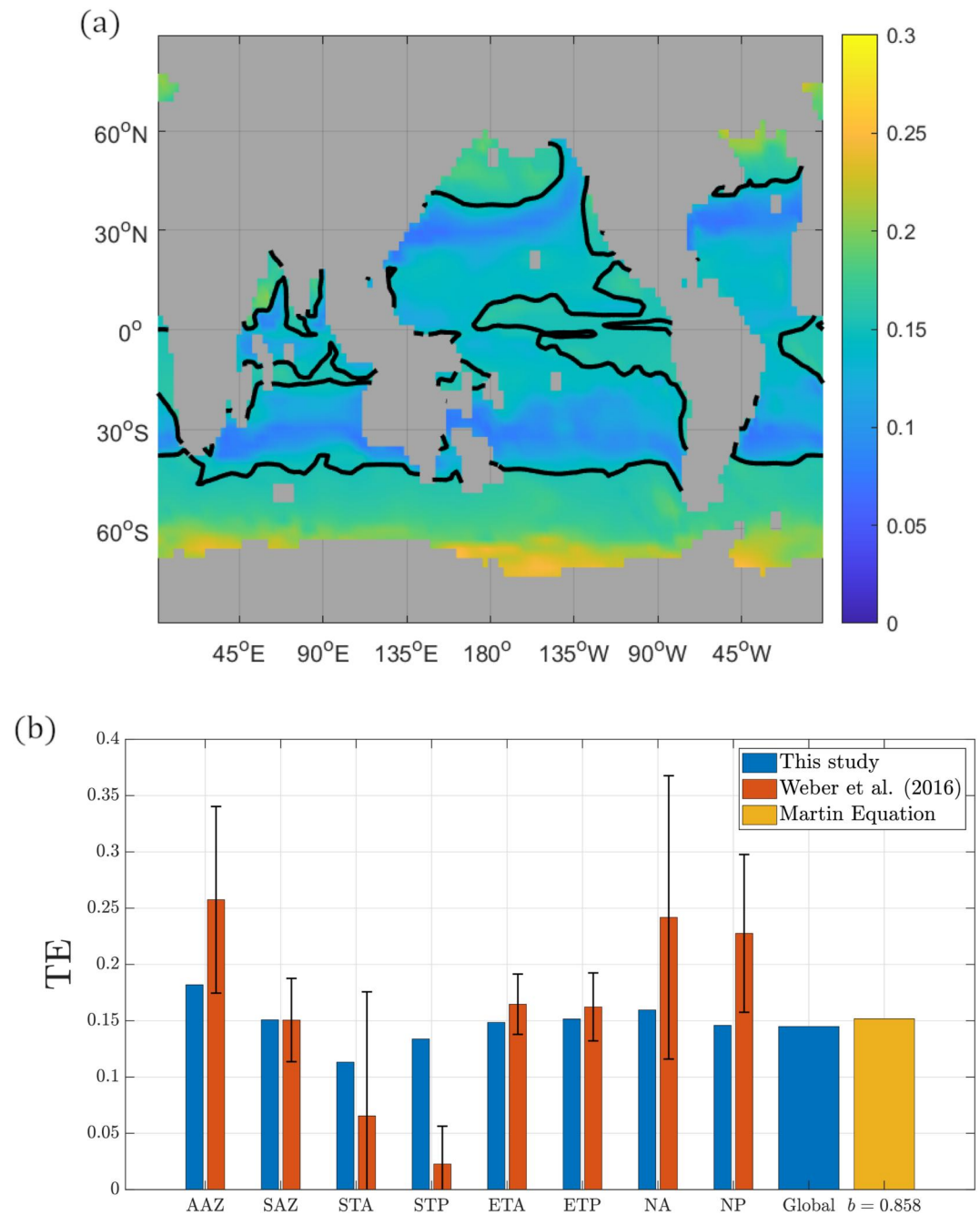


Figure 2. Annual mean transfer efficiency (TE), when detritus is not transported by the ocean circulation. Top: (a) TE for a seasonal b^{model} —the solid black contour lines represents the TE computed from the Martin curve for $b = 0.858$. Bottom: (b) annual mean TE in each ocean province (definition in Supporting Information S1) using data from this study (blue bars) and the data-constrained modeling study (Weber et al., 2016) (red bars, with intervals indicating the uncertainty in their analysis), with the yellow bar showing the value for TE as estimated using the Martin curve (Supporting Information S1) for $b = 0.858$. Note that the province definition in this study and in the data-constrained modeling study (Weber et al., 2016) are slightly different (see Supporting Information S1).

The results in Figures 2 and 3 demonstrate that spatial variability in TE may not emerge uniquely from spatially varying processes, such as temperature-dependent remineralization, but could also arise from the coupling between seasonally varying processes, therefore challenging the interpretation of spatial variability in annual mean TE data sets.

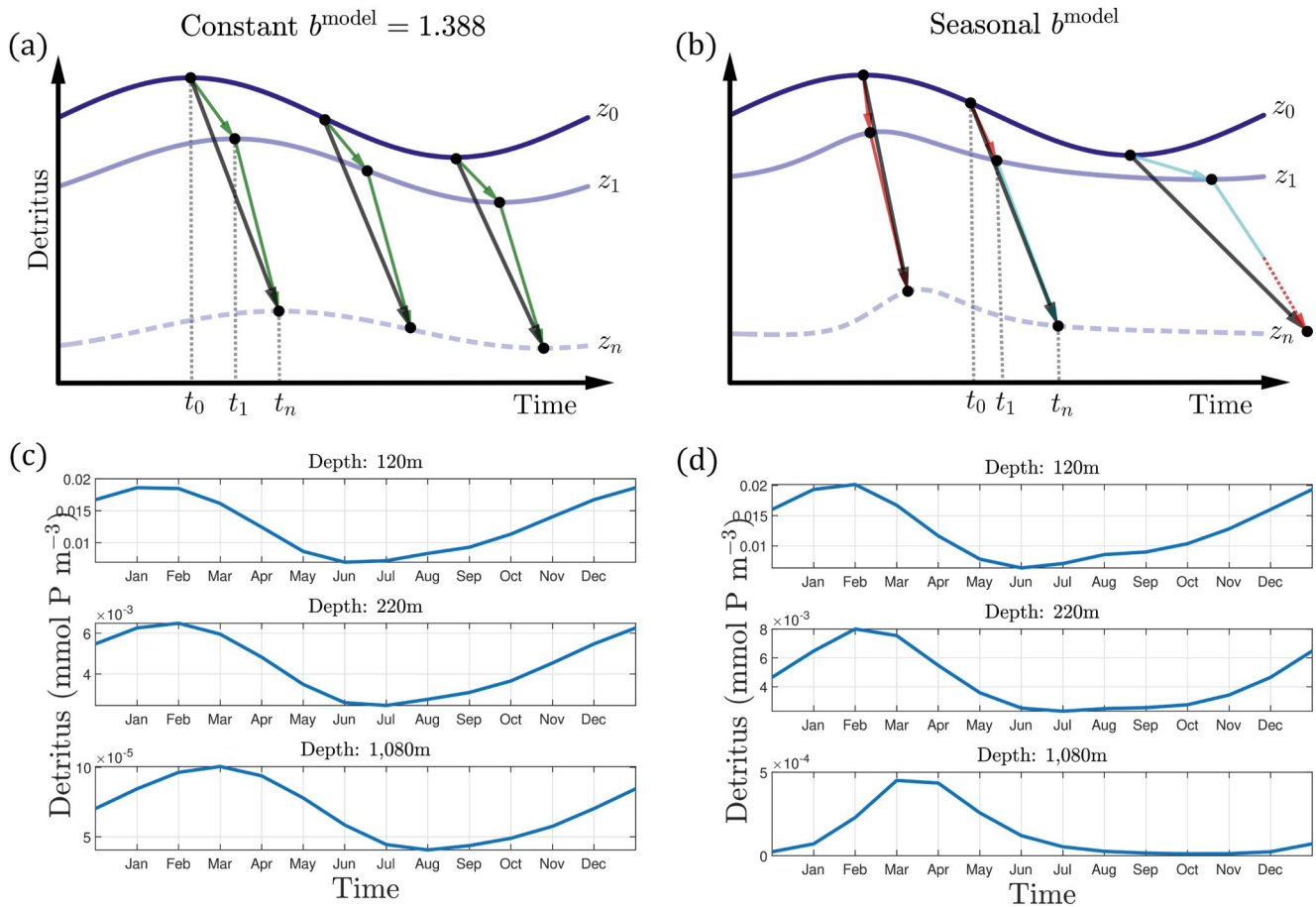


Figure 3. Exported detritus attenuation in constant and seasonal attenuation scenarios, when detritus is not transported by the ocean circulation. Top: schematic representation showing how detritus is attenuated in a non-seasonal scenario (a) and when seasonality is present (b). In panel (a), detritus that is at the export depth z_0 at an instant t_0 would be uniformly attenuated, reaching a depth z_1 at an instant t_1 , as shown by the green arrow. Then, the attenuation continues at a uniform rate, with sinking speed increasing as a function of depth, so that the remaining detritus reaches the transfer depth z_n at an instant t_n . As both attenuation and sinking are constant in time, this process is independent of the starting point, as shown by the dark gray arrows, which are parallel to each other. In panel (b), the attenuation varies seasonally and hence the journey of detritus is dependent on time of the year. For instance, detritus that is at the export depth z_0 at the instant t_0 depicted would go through a lower attenuation, sinking at a faster rate until it reaches z_1 at the instant t_1 , as shown by the red arrow. This is then followed by a faster attenuation, when detritus sinks at a slower rate, until it reaches the transfer depth z_n at an instant t_n , as shown by the light blue arrow. For detritus leaving z_0 at other times, the attenuation journey would be different, and hence the gray arrows are not parallel. Bottom: modeled time series for detritus concentration in the South Atlantic (43.59°S, 29.53°W) at different depths for a constant $b^{\text{model}} = 1.388$ (c) and a seasonal b^{model} (d), demonstrating the phenomena described in panels (a) and (b) respectively. Note the changing scale of the axes in panels (c) and (d).

3.2. Seasonality Reconciles Contrasting Spatial Patterns of Observed Transfer Efficiency

The seasonal variability in attenuation can also explain apparent conflicts between existing estimates for TE (Cram et al., 2018; DeVries & Weber, 2017; Guidi et al., 2015; Henson et al., 2012; Marsay et al., 2015; Weber et al., 2016). The existence of a seasonal cycle itself implies that if sampling the same location in the ocean at different times of the year, estimates of flux attenuation and TE are likely to be quite different. In addition, the seasonal cycle could be highly episodic: as ship-board observations are collected for very short periods, sampling might occur in for example, an overall period of slow sinking with occasional short-lived peaks. Hence, compiling short-duration observations from several years made at different times of the year and at different locations assuming they represent a single snapshot of the ocean BCP state is likely to be misleading.

Previous suggestions (Marsay et al., 2015) on how to reconcile these divergent estimates focused on the possibility of a fast upper mesopelagic attenuation followed by slow attenuation in the deep ocean in warm waters, with the converse happening in cold waters, but did not consider the role of seasonality and variability in flux attenuation and sinking speeds, nor the implicit steady-state assumption that is inherent in most reports of short-

term observations of sinking POC (Giering et al., 2017). Although this temperature-attenuation relationship was later observed in a data-constrained model analysis (DeVries & Weber, 2017), the existence of this phenomenon was not enough to generate the high-latitude low-TE patterns (DeVries & Weber, 2017).

Here we argue that the different time scales introduced by temporal variability of attenuation and sinking provides an explanation for the high-latitude low-TE pattern. In a situation where flux attenuation varies seasonally, sufficiently frequent sampling to allow representation of global annual averages is not typically viable with ship-based observations.

To test whether this mechanism could provide an answer to the contrasting pattern of TE obtained in the study using sediment trap and Thorium-derived fluxes (Henson et al., 2012), we reproduced their sampling methodology as closely as possible using our model simulation results, taking into consideration the limitations of our modeling framework (see Supporting Information S1).

Figure 4 shows the results of reproducing the sediment trap and Thorium-derived fluxes study (Henson et al., 2012) using the same model data used to produce Figure 2. Instead of computing the annual average export and transfer flux to produce a TE map as in Figure 2a, we sampled the model data at locations and dates that best matched their approach (see Supporting Information S1 for details). Specifically, we randomly sampled a total of 150 high and low latitude locations as shown in Figure 4a, from which we took annual fluxes at 1,000 m and seasonally averaged (for the periods covered in their data set) export fluxes at 120 m, with the corresponding mean surface (0–120 m) temperature for the same period. We then used these data to compute TE at each sampled location, which was correlated (both linearly and exponentially, see Supporting Information S1) with the surface mean temperature at the same location, as shown in Figure 4b. This process was repeated 10,000 times to quantify the uncertainty, giving a normally distributed R^2 with mean 0.79 and variance 0.033 for the exponential regression (see Supporting Information S1). The mean correlation maps (linear and exponential) were then used to produce global TE maps. The resulting map for the exponential fit is shown in Figure 4b (see Supporting Information S1 for the linear fit map). This provides a fairly reasonable explanation to the differences with the sediment trap-based study (Marsay et al., 2015), showing a low TE in high latitudes and a higher TE in the tropics and subtropics, hence suggesting that the seasonal signal for export in these periods were enough to reverse the TE pattern from Figure 2a—even though both TE maps were generated from the same data. A similar result was obtained when using the mean upper-mesopelagic (120–540 m) temperature, which is shown in the Supporting Information S1. We note that a correlation between TE and surface temperature is not found if we instead use TE data from a model run with a non-seasonal, constant flux attenuation. In this case, the linear regression essentially provides a horizontal line, as shown in Figure S13 in Supporting Information S1 for $b^{\text{model}} = 1.388$, evidencing the need of seasonality in flux attenuation to explain the high-latitude low-TE pattern.

Our analysis demonstrates that temporally inconsistent data compilations could lead to differing conclusions, particularly when generalized to non-sampled parts of the ocean. In this case, measurements that have some consistency in date (i.e., from around the same time of the year) and location might be required to draw robust conclusions on the processes driving the BCP.

3.3. Caveats in This Study

This study has some caveats, which are informative and offer opportunities for further investigations. These include the use of a coarse resolution model which does not resolve small scale processes (although they are parameterized), as well as a periodically repeating circulation. However, we note that these methods have been successfully employed in a variety of studies (DeVries & Weber, 2017; Khaliwala, 2007; Kriest & Oschlies, 2013; Niemeyer et al., 2019; Weber et al., 2016).

Another limitation is in the use of a non-mechanistic seasonal cycle in flux attenuation, which is based on very limited evidence (Guidi et al., 2015), and is the simplest representation of seasonal variation in attenuation. In reality, it may vary in both amplitude and phase with location, but the details are still uncertain. The shape (i.e., how peaked) of the attenuation time series might, at some locations, be quite different from the simple smooth signal (see Materials and Methods) considered in this work. Although the true shape could be different, this does not affect the main results. The important feature is the lag between POC export and attenuation which is where we believe the scientific attention should now focus.

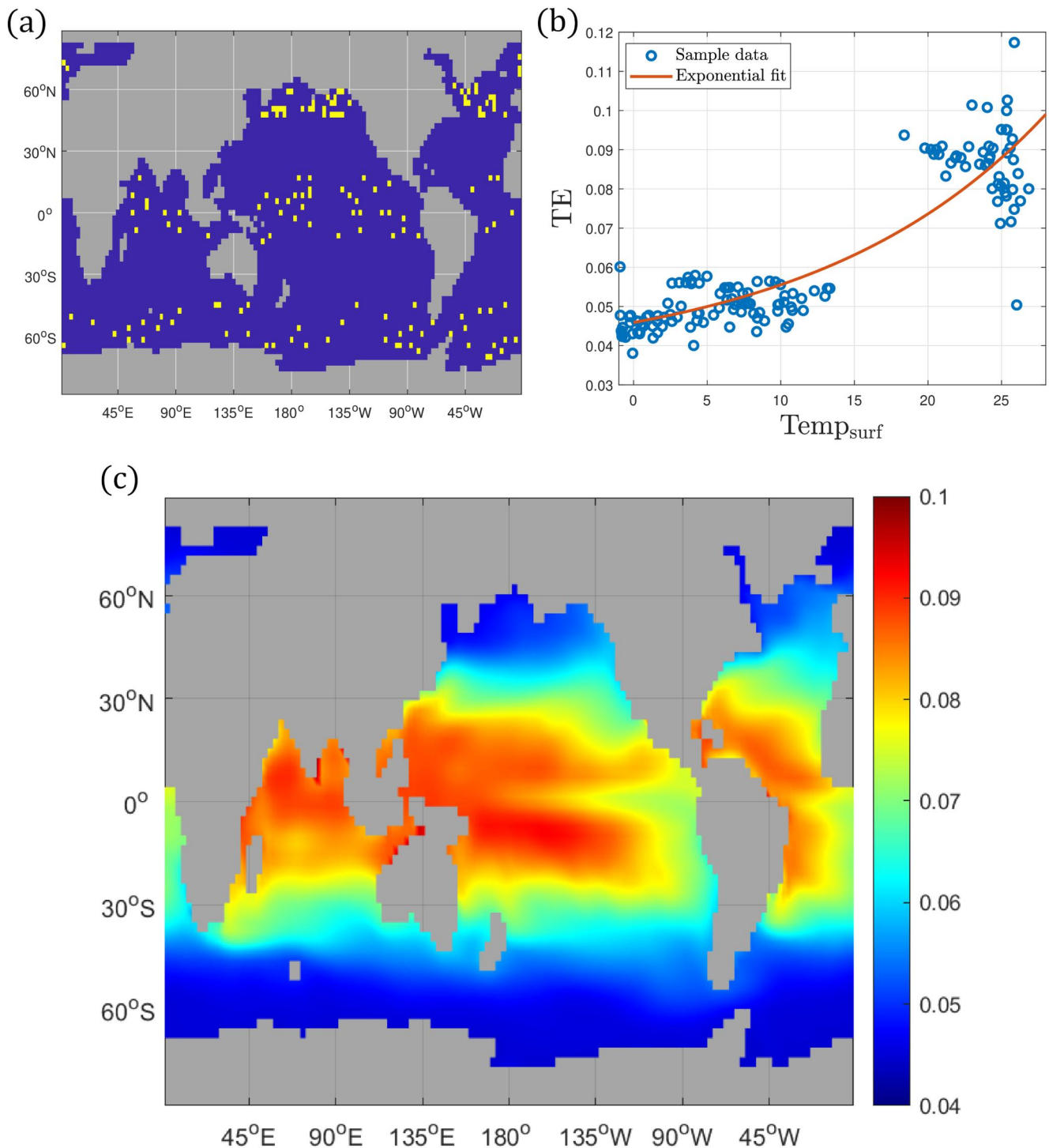


Figure 4. Time-discrete sampling with seasonal variability in attenuation can produce contrasting spatial patterns in the true annual mean transfer efficiency (TE) shown in Figure 2a, providing an explanation to reconcile previous sediment trap studies (Guidi et al., 2015; Henson et al., 2012). Top: (a) export and transfer fluxes were sampled randomly, and (b) a nonlinear (exponential) regression of the resulting TE against the surface (0–120 m) temperature was performed. This procedure was repeated 10,000 times and the resulting parameterization was used to compute the TE map shown in panel (c).

We also note that there is evidence that mixing and upwelling can affect estimates of the flux attenuation, particularly at high latitudes (de Melo Viríssimo et al., 2022; Kriest & Oschlies, 2011; Niemeier et al., 2019). This suggests that such an effect might be present in the data used to constrain the flux attenuation b^{model} (and therefore in b^{model} itself), highlighting the need to understand both biological and physical influences that affect the shape and phase of the flux attenuation seasonality.

The results in this study also ignore the effects, however small, of circulation in the transport of detritus, meaning that it can only move vertically due to gravity, but is not transported laterally nor vertically by mixing or upwelling. This is only a minor hypothesis which has been deliberately used in other studies (Pasquier et al., 2023), and in the diagnostics of b in the data-constrained modeling study (Weber et al., 2016). However, adding the effect of the circulation in the advection of would change slightly the fluxes and introduce minor spatial patterns in TE (de Melo Viríssimo et al., 2022), therefore preventing a clean diagnostic of the contribution due to the presence of seasonality. Furthermore, this hypothesis has three important benefits: first, it demonstrates this effect can take place even with strictly local influence; Second, this approach removes any uncertainties when quantifying the ratio of fluxes at two depths in a single location (where the deeper one may average a larger area in reality); Third, since the flux attenuation b^{model} was inferred from in-situ observations (where circulation is inevitably present), our approach prevents the circulation effects on b^{model} from being accounted for twice.

These model limitations, however, do not affect the purpose of this study, which is not to reproduce reality *ipsis literis* but to test a hypothesis and demonstrate a phenomenon. Hence, it should not be taken as an intended accurate depiction of the real seasonal cycle, nor be reproduced in models as such, despite being successful in reconciling previous literature results while highlighting an important but neglected phenomenon. Note that it also ignores the fact that a real flux attenuation time series might show inter-annual variability, and hence its scope is limited to the hypothesis tested in this study.

Lastly, the analysis presented in Section 3.2 does not exclude the possibility of some systematic biases in the combination of Thorium and deep sediment trap data of Henson et al. (2012). However, it is unclear whether such biases (if existent) would impact qualitatively the high-latitude low-TE pattern shown in their study.

4. Summary and Conclusion

We showed that the addition of a seasonal cycle in the flux attenuation has at least three striking consequences for the global patterns of annual TE. First, spatial variability is generated despite both flux attenuation and sinking speed being spatially homogeneous at each instant of time. Second, the emerging spatial pattern in annual TE is highly similar to that reported in the literature (Cram et al., 2018; DeVries & Weber, 2017; Marsay et al., 2015; Weber et al., 2016). Third, accounting for the seasonality allows for the high-latitude high-TE map (Marsay et al., 2015) to be reconciled with the alternative high-latitude low-TE pattern (Henson et al., 2012).

These results suggest that seasonal variability in flux attenuation and sinking speed is a route for generating spatial variability in annual TE, as a natural emerging property of the system dynamics. This is different from imposing a spatially varying TE or b^{model} a priori, and is the simple consequence of the coupling between two seasonal time series (i.e., flux attenuation and export of organic material; or equivalently, sinking speed and detritus concentration) to obtain fluxes - excluding the transport due to circulation.

This has also implications for CMIP-class models run under anthropogenic forcing: changes in climate forcing might trigger changes in the seasonal cycle and hence impact carbon fluxes and spatial variability in TE too. Hence, assuming a fixed spatial and temporal pattern in flux attenuation limits the model assessment of the BCP and sequestration under climate change in the IPCC scenarios. This is particularly important as previous numerical studies have demonstrated that changes in the phase impact the amount of carbon that is transferred to the deep ocean (de Melo Viríssimo et al., 2022), meaning that we need to understand the causes of the lag between POC export and attenuation to have more confidence in predictions. We note that most CMIP6 models adopt constant (in time, space and depth) sinking speeds (Henson et al., 2022; Wilson et al., 2022), with only two models using a variable formulation: one has a sinking speed that is constant in time but increases with depth (Aumont et al., 2015), and another has a sinking speed that varies according to the nutrient stress (Vichi et al., 2007). Therefore, incorporating mechanistic-based models for sinking particles is an open challenge for the CMIP7 generation and beyond.

Finally, observationally resolving the temporal scales of fluxes and related processes such as sinking speed, remineralization, and metabolic rates would represent a big step toward a better quantification and understanding of the BCP, and particularly the seasonality of export and attenuation. Model estimates of flux are difficult to validate due to sparsity of observations (Weber et al., 2016), not only spatially but especially temporally, but there is a potential for autonomous observations to fill in some of the gaps - particularly the seasonal variability in attenuation (Bol et al., 2018; Brewin et al., 2021; Briggs et al., 2020; Claustre et al., 2020; Dall'Olmo & Mork, 2014). In addition, the use of data-constrained models and machine learning (Clements et al., 2022) offer some hope and can be a fruitful avenue to extract seasonal information from the more abundant data existent for other tracers and processes, and should be one of the top priorities for the biogeochemical and climate modeling communities over the next few years.

Conflict of Interest

The authors declare no conflict of interest.

Data Availability Statement

All model output used in this work is freely available online on Zenodo (de Melo Viríssimo et al., 2023). The flux attenuation data used to generate Figure 1 is available as supporting information in the referred manuscript (Guidi et al., 2015). The data (Weber et al., 2016) used to generate part of Figure 2b is available on Bitbucket (Cram, 2018; Cram et al., 2018). All figures in this work were generated by the authors. Figures 3a and 3b were generated using the software GeoGebra (Hohenwarter et al., 2018). Figure S1a in Supporting Information S1 was generated using the MATLAB package M map (Pawlowicz, 2020).

Acknowledgments

The authors thank the two anonymous reviewers for their valuable feedback, which helped to improve this manuscript, and the editors and editorial staff at GRL. F.d.M.V. thank Dr Raffaele Bernadello for his support in setting up the MOPS model back in 2019. The work in this manuscript was partially conducted at the National Oceanography Centre in Southampton, United Kingdom. This work was funded by: an European Research Council Consolidator Grant (GOCART, agreement number 724416) in support of F.d.M.V. and S.A.H.; by a Large Grant from the UK Natural Environment Research Council (COMICS, agreement numbers NE/M020835/1 and NE/M020835/2) in support of F.d.M.V., A.P.M. and S.A.H.; and by a UK Natural Environment Research Council RoSES programme Grant (CUSTARD, agreement number NE/P021247/2) in support of F.d.M.V., A. P.M. and S.A.H. J.D.W. acknowledges support from the AXA Research Fund.

References

- Alcolombri, U., Peaudecerf, F., Fernandez, V., Behrendt, L., Soo Lee, K., & Stocker, R. (2021). Sinking enhances the degradation of organic particles by marine bacteria. *Nature Geosciences*, 14(10), 775–780. <https://doi.org/10.1038/s41561-021-00817-x>
- Aumont, O., Ethé, C., Tagliabue, A., Bopp, L., & Gehlen, M. (2015). Pisces-v2: An ocean biogeochemical model for carbon and ecosystem studies. *Geoscientific Model Development*, 8(8), 2465–2513. <https://doi.org/10.5194/gmd-8-2465-2015>
- Berelson, W. M. (2001). The flux of particulate organic carbon into the ocean interior: A comparison of four U.S. JGOFS regional studies. *Oceanography*, 14(4), 59–67. <https://doi.org/10.5670/oceanog.2001.07>
- Bol, R., Henson, S. A., Rumyantseva, A., & Briggs, N. (2018). High-frequency variability of small-particle carbon export flux in the northeast atlantic. *Global Biogeochemical Cycles*, 32(12), 1803–1814. <https://doi.org/10.1029/2018GB005963>
- Brewin, R. J., Sathyendranath, S., Platt, T., Bouman, H., Ciavatta, S., Dall'Olmo, G., et al. (2021). Sensing the ocean biological carbon pump from space: A review of capabilities, concepts, research gaps and future developments. *Earth-Science Reviews*, 217, 103604. <https://doi.org/10.1016/j.earscirev.2021.103604>
- Briggs, N., Dall'Olmo, G., & Claustre, H. (2020). Major role of particle fragmentation in regulating biological sequestration of CO₂ by the oceans. *Science*, 367(6479), 791–793. <https://doi.org/10.1126/science.aay1790>
- Buesseler, K. O., Lamborg, C. H., Boyd, P. W., Lam, P. J., Trull, T. W., Bidigare, R. R., et al. (2007). Revisiting carbon flux through the ocean's twilight zone. *Science*, 316(5824), 567–570. <https://doi.org/10.1126/science.1137959>
- Claustre, H., Johnson, K. S., & Takeshita, Y. (2020). Observing the global ocean with biogeochemical-argo. *Annual Review of Marine Science*, 12(1), 23–48. <https://doi.org/10.1146/annurev-marine-010419-010956>
- Clements, D. J., Yang, S., Weber, T., McDonnell, A. M. P., Kiko, R., Stemmann, L., & Bianchi, D. (2022). Constraining the particle size distribution of large marine particles in the global ocean with in situ optical observations and supervised learning. *Global Biogeochemical Cycles*, 36(5), e2021GB007276. <https://doi.org/10.1029/2021GB007276>
- Conte, M. H., Ralph, N., & Ross, E. H. (2001). Seasonal and interannual variability in deep ocean particle fluxes at the oceanic flux program (OFP)/Bermuda Atlantic time series (bats) site in the western Sargasso Sea near Bermuda. *Deep Sea Research Part II: Topical Studies in Oceanography*, 48(8), 1471–1505. [https://doi.org/10.1016/S0967-0645\(00\)00150-8](https://doi.org/10.1016/S0967-0645(00)00150-8)
- Cram, J. A. (2018). Model output used in the manuscript “the role of particle size, ballast, temperature, and oxygen in the sinking flux to the deep sea”. Retrieved from <https://bitbucket.org/ohnoplus/prism-transfer-efficiency>
- Cram, J. A., Weber, T., Leung, S. W., McDonnell, A. M. P., Liang, J.-H., & Deutsch, C. (2018). The role of particle size, ballast, temperature, and oxygen in the sinking flux to the deep sea. *Global Biogeochemical Cycles*, 32(5), 858–876. <https://doi.org/10.1029/2017GB005710>
- Dall'Olmo, G., & Mork, K. A. (2014). Carbon export by small particles in the Norwegian Sea. *Geophysical Research Letters*, 41(8), 2921–2927. <https://doi.org/10.1002/2014GL059244>
- de Melo Viríssimo, F., Martin, A. P., & Henson, S. A. (2022). Influence of seasonal variability in flux attenuation on global organic carbon fluxes and nutrient distributions. *Global Biogeochemical Cycles*, 36(2), e2021GB007101. <https://doi.org/10.1029/2021GB007101>
- de Melo Viríssimo, F., Martin, A. P., Henson, S. A., & Wilson, J. D. (2023). Model output used in the manuscript “Seasonality in carbon flux attenuation explains spatial variability in transfer efficiency” (v1.0). *Zenodo*. <https://doi.org/10.5281/zenodo.7514129>
- DeVries, T., Primeau, F., & Deutsch, C. (2012). The sequestration efficiency of the biological pump. *Geophysical Research Letters*, 39(13). <https://doi.org/10.1029/2012GL051963>
- DeVries, T., & Weber, T. (2017). The export and fate of organic matter in the ocean: New constraints from combining satellite and oceanographic tracer observations. *Global Biogeochemical Cycles*, 31(3), 535–555. <https://doi.org/10.1002/2016GB005551>
- Francois, R., Honjo, S., Krishfield, R., & Manganini, S. (2002). Factors controlling the flux of organic carbon to the bathypelagic zone of the ocean. *Global Biogeochemical Cycles*, 16(4), 34–1–34–20. <https://doi.org/10.1029/2001GB001722>

- Giering, S. L. C., Sanders, R., Martin, A. P., Henson, S. A., Riley, J. S., Marsay, C. M., & Johns, D. G. (2017). Particle flux in the oceans: Challenging the steady state assumption. *Global Biogeochemical Cycles*, 31(1), 159–171. <https://doi.org/10.1002/2016GB005424>
- Guidi, L., Legendre, L., Reygondeau, G., Uitz, J., Stemann, L., & Henson, S. A. (2015). A new look at ocean carbon remineralization for estimating deepwater sequestration. *Global Biogeochemical Cycles*, 29(7), 1044–1059. <https://doi.org/10.1002/2014GB005063>
- Henson, S. A., Briggs, N., Carvalho, F., Manno, C., Mignot, A., & Thomalla, S. (2023). A seasonal transition in biological carbon pump efficiency in the northern scotia sea, southern ocean. *Deep Sea Research Part II: Topical Studies in Oceanography*, 208, 105274. <https://doi.org/10.1016/j.dsr2.2023.105274>
- Henson, S. A., Laufkötter, C., Leung, S., Giering, S. L. C., Palevski, H. I., & Cavan, E. L. (2022). Uncertain response of ocean biological carbon export in a changing world. *Nature Geosciences*, 15(4), 248–254. <https://doi.org/10.1038/s41561-022-00927-0>
- Henson, S. A., Sanders, R., & Madsen, E. (2012). Global patterns in efficiency of particulate organic carbon export and transfer to the deep ocean. *Global Biogeochemical Cycles*, 26(1). <https://doi.org/10.1029/2011GB004099>
- Hohenwarter, M., Borchers, M., Ancsin, G., Bencze, B., Blossier, M., Éliás, J., et al. (2018). GeoGebra 5.0.507.0. <http://www.geogebra.org>
- Khatiwal, S. (2007). A computational framework for simulation of biogeochemical tracers in the ocean. *Global Biogeochemical Cycles*, 21(3). <https://doi.org/10.1029/2007GB002923>
- Khatiwal, S. (2018). samarkhatiwal/tmm: Version 2.0 of the transport matrix method software (2018, may 13). *Zenodo*. <https://doi.org/10.5281/zenodo.1246300>
- Khatiwal, S., Visbeck, M., & Cane, M. A. (2005). Accelerated simulation of passive tracers in ocean circulation models. *Ocean Modelling*, 9(1), 51–69. <https://doi.org/10.1016/j.ocemod.2004.04.002>
- Kienast, S. S., & Torfstein, A. (2022). Evaluation of biological carbon pump metrics in the subtropical gulf of aqaba, northern red sea. *Global Biogeochemical Cycles*, 36(10). e2022GB007452. <https://doi.org/10.1029/2022GB007452>
- Kriest, I., Khatiwal, S., & Oschlies, A. (2010). Towards an assessment of simple global marine biogeochemical models of different complexity. *Progress in Oceanography*, 86(3), 337–360. <https://doi.org/10.1016/j.pocean.2010.05.002>
- Kriest, I., & Oschlies, A. (2011). Numerical effects on organic-matter sedimentation and remineralization in biogeochemical ocean models. *Ocean Modelling*, 39(3), 275–283. <https://doi.org/10.1016/j.ocemod.2011.05.001>
- Kriest, I., & Oschlies, A. (2013). Swept under the carpet: Organic matter burial decreases global ocean biogeochemical model sensitivity to remineralization length scale. *Biogeosciences*, 10(12), 8401–8422. <https://doi.org/10.5194/bg-10-8401-2013>
- Kriest, I., Oschlies, A., & Khatiwal, S. (2012). Sensitivity analysis of simple global marine biogeochemical models. *Global Biogeochemical Cycles*, 26(2). <https://doi.org/10.1029/2011GB004072>
- Kriest, I., Sauerland, V., Khatiwal, S., Srivastav, A., & Oschlies, A. (2017). Calibrating a global three-dimensional biogeochemical ocean model (mops-1.0). *Geoscientific Model Development*, 10(1), 127–154. <https://doi.org/10.5194/gmd-10-127-2017>
- Kwon, E., Primeau, F., & Sarmiento, J. (2009). The impact of remineralization depth on the air–sea carbon balance. *Nature Geosciences*, 2(9), 630–635. <https://doi.org/10.1038/ngeo612>
- Lima, I. D., Lam, P. J., & Doney, S. C. (2014). Dynamics of particulate organic carbon flux in a global ocean model. *Biogeosciences*, 11(4), 1177–1198. <https://doi.org/10.5194/bg-11-1177-2014>
- Lutz, M., Dunbar, R., & Caldeira, K. (2002). Regional variability in the vertical flux of particulate organic carbon in the ocean interior. *Global Biogeochemical Cycles*, 16(3), 11–1–11–18. <https://doi.org/10.1029/2000GB001383>
- Maier-Reimer, E., Mikolajewicz, U., & Winguth, A. (1996). Future ocean uptake of CO₂: Interaction between ocean circulation and biology. *Climate Dynamics*, 12(10), 711–722. <https://doi.org/10.1007/s003820050138>
- Marsay, C. M., Sanders, R. J., Henson, S. A., Pabortsava, K., Achterberg, E. P., & Lampitt, R. S. (2015). Attenuation of sinking particulate organic carbon flux through the mesopelagic ocean. *Proceedings of the National Academy of Sciences*, 112(4), 1089–1094. <https://doi.org/10.1073/pnas.1415311112>
- Martin, J. H., Knauer, G. A., Karl, D. M., & Broenkow, W. W. (1987). Vertex: Carbon cycling in the northeast pacific. *Deep Sea Research Part A. Oceanographic Research Papers*, 34(2), 267–285. [https://doi.org/10.1016/0198-0149\(87\)90086-0](https://doi.org/10.1016/0198-0149(87)90086-0)
- Middelburg, J. J. (2019). *Marine carbon biogeochemistry: A primer for earth system scientists* (1st ed.). Springer International Publishing.
- Niemeyer, D., Kriest, I., & Oschlies, A. (2019). The effect of marine aggregate parameterisations on nutrients and oxygen minimum zones in a global biogeochemical model. *Biogeosciences*, 16(15), 3095–3111. <https://doi.org/10.5194/bg-16-3095-2019>
- Nowicki, M., DeVries, T., & Siegel, D. A. (2022). Quantifying the carbon export and sequestration pathways of the ocean's biological carbon pump. *Global Biogeochemical Cycles*, 36(3), e2021GB007083. <https://doi.org/10.1029/2021GB007083>
- Pasquier, B., Holzer, M., Chamberlain, M. A., Matear, R. J., Bindoff, N. L., & Primeau, F. W. (2023). Optimal parameters for the ocean's nutrient, carbon, and oxygen cycles compensate for circulation biases but replumb the biological pump. *Biogeosciences*, 20(14), 2985–3009. <https://doi.org/10.5194/bg-20-2985-2023>
- Pawlowicz, R. (2020). “M map: A mapping package for MATLAB”, version 1.4m [Computer software]. www.eoas.ubc.ca/~rich/map.html
- Saba, G. K., Burd, A. B., Dunne, J. P., Hernández-León, S., Martin, A. H., Rose, K. A., et al. (2021). Toward a better understanding of fish-based contribution to ocean carbon flux. *Limnology & Oceanography*, 66(5), 1639–1664. <https://doi.org/10.1002/lno.11709>
- Vichi, M., Pinardi, N., & Masina, S. (2007). A generalized model of pelagic biogeochemistry for the global ocean ecosystem. Part I: Theory. *Journal of Marine Systems*, 64(1), 89–109. <https://doi.org/10.1016/j.jmarsys.2006.03.006>
- Volk, T., & Hoffert, M. I. (2013). Ocean carbon pumps: Analysis of relative strengths and efficiencies in ocean-driven atmospheric CO₂ changes. In *The carbon cycle and atmospheric CO₂: Natural variations archean to present* (pp. 99–110). American Geophysical Union (AGU). <https://doi.org/10.1029/GM032p0099>
- Weber, T., Cram, J. A., Leung, S. W., DeVries, T., & Deutsch, C. (2016). Deep ocean nutrients imply large latitudinal variation in particle transfer efficiency. *Proceedings of the National Academy of Sciences*, 113(31), 8606–8611. <https://doi.org/10.1073/pnas.1604414113>
- Wilson, J. D., Andrews, O., Katavouta, A., de Melo Virissimo, F., Death, R. M., Adloff, M., et al. (2022). The biological carbon pump in CMIP6 models: 21st century trends and uncertainties. *Proceedings of the National Academy of Sciences*, 119(29), e2204369119. <https://doi.org/10.1073/pnas.2204369119>
- Wilson, J. D., Barker, S., Edwards, N. R., Holden, P. B., & Ridgwell, A. (2019). Sensitivity of atmospheric CO₂ to regional variability in particulate organic matter remineralization depths. *Biogeosciences*, 16(14), 2923–2936. <https://doi.org/10.5194/bg-16-2923-2019>